

## Structure of the Solvated Zinc(II), Cadmium(II), and Mercury(II) Ions in *N,N*-Dimethylthioformamide Solution

Christina M. V. Stålhandske,<sup>†</sup> Ingmar Persson,<sup>\*,†</sup> Magnus Sandström,<sup>\*,‡</sup> and Ewa Kamienska-Piotrowicz<sup>†,§</sup>

Department of Chemistry, Swedish University of Agricultural Sciences, P.O. Box 7015, S-750 07 Uppsala, Sweden, and Department of Chemistry, Royal Institute of Technology, S-100 44 Stockholm, Sweden

Received November 6, 1996<sup>⊗</sup>

By means of large-angle X-ray scattering zinc(II) and mercury(II) ions in *N,N*-dimethylthioformamide solution are found to coordinate to four *N,N*-dimethylthioformamide molecules with Zn–S and Hg–S bond distances of 2.362(5) and 2.527(6) Å, respectively. The intermediate divalent ion in group 12, cadmium, is solvated by six *N,N*-dimethylthioformamide molecules with a Cd–S bond distance of 2.69(1) Å. Raman and far-infrared spectra have been recorded and assigned for the solvated ions both in solution and in the solid state. The character of the bonds to the metal ion is discussed in order to explain the lower coordination numbers of the zinc and mercury(II) ions.

### Introduction

The divalent d<sup>10</sup> ions of group 12, Zn<sup>2+</sup>, Cd<sup>2+</sup>, and Hg<sup>2+</sup>, display a large variety of coordination geometries. The flexibility of the zinc ion is of vital importance for its role in the active site of numerous metalloenzymes and in many other important biochemical processes.<sup>1</sup> A recent survey of crystal structures shows prevalent tetrahedral four-coordination for zinc compounds but octahedral six-coordination in the majority of cadmium structures.<sup>2</sup> Mercury(II) often displays linear two-coordination or tetrahedral four-coordination in its complexes.<sup>3</sup> With monodentate ligands, however, as is the case for solvated metal ions, octahedral six-coordination is common in zinc complexes and also occurs for mercury(II), e.g. in its hexasolvates of water, dimethyl sulfoxide, pyridine 1-oxide, and pyridine.<sup>4–8</sup>

A theoretical study has shown the energy gain to be small between four- and six-coordinated hydrated Zn<sup>2+</sup> ions.<sup>2</sup> Steric repulsion between the ligands is more important for the smaller zinc ion, and with the bulky monodentate oxygen-donor solvent tetramethylurea zinc forms four-coordinated solvates, although six-coordination is maintained with the larger Cd<sup>2+</sup> ion.<sup>9</sup>

Mercury(II), cadmium, and in particular zinc ions often show tetrahedral four-coordination with soft sulfur-donor ligands, for

example with sulfides and most alkyl xanthate, *O,O*-dialkyl dithiophosphate and *N,N*-dialkyldithiocarbamate ions.<sup>3,10,11</sup> A special feature of mercury(II) complexes with soft donor ligands is that two strong collinear bonds are frequently formed, often combined with weak equatorial contacts or secondary bonds to distant atoms,<sup>12</sup> sometimes giving rise to an axially compressed octahedron around the central mercury(II) ion in the solid state.<sup>3</sup> For mercury(II), a theoretical study shows that vibronic coupling destabilizes a regular octahedral coordination geometry.<sup>13</sup> This destabilization is found to be stronger with sulfur than with oxygen ligands, and no structure with regular coordination of six sulfur ligands around mercury(II) has been found experimentally.

Evidently, increasing covalency of the metal–ligand bond strongly influences the coordination of the group 12 ions, and it was therefore of interest to study the effect of a soft donor ligand. The *N,N*-dimethylthioformamide molecule is a monodentate sulfur donor with a high dipole moment,  $\mu = 4.44$  D.<sup>14</sup> It is also one of very few sulfur donor solvents with a sufficiently high permittivity,  $\epsilon = 47.5$ ,<sup>15</sup> to sustain concentrated electrolyte solutions of divalent ions. Crystalline *N,N*-dimethylthioformamide solvates of zinc and cadmium ions have been prepared from saturated solutions with noncoordinating anions.<sup>16</sup> Single-crystal X-ray diffraction studies showed four- and six-coordination around the Zn<sup>2+</sup> and Cd<sup>2+</sup> ions, respectively. For mercury(II), however, only a two-coordinated crystalline solvate could be obtained when *N,N*-dimethylthioformamide was added to an acetonitrile solution; our attempts to obtain crystals from a saturated *N,N*-dimethylthioformamide solution of mercury(II) perchlorate failed.<sup>16</sup> However, in a discussion of how the chemical bonding influences the coordination of a metal ion, solution studies of the structure and of thermodynamic properties are preferable. In the crystalline state intermolecular interactions

<sup>†</sup> Swedish University of Agricultural Sciences.

<sup>‡</sup> Royal Institute of Technology.

<sup>§</sup> Present address: Department of Physical Chemistry, Technical University of Gdansk, ul. Gabriela Narutowicza 11/12, PL-80-952 Gdansk-Wrzeszcz, Poland.

<sup>⊗</sup> Abstract published in *Advance ACS Abstracts*, June 1, 1997.

- (1) Siegel, H.; Martin, R. B. *Chem. Soc. Rev.* **1994**, 83.
- (2) Bock, C. W.; Kaufman Katz, A.; Glusker, J. P. *J. Amer. Chem. Soc.* **1995**, *117*, 3754.
- (3) (a) Prince, R. H. In *Comprehensive Coordination Chemistry*; Wilkinson, G., Gillard, R. D., McCleverty, J. A., Eds.; Pergamon: Oxford, England, 1987; Vol. 5, Chapter 56.1, p 925. (b) Brodersen, K.; Hummel, H.-U. *Ibid.*, Vol. 5, Chapter 56.2, p 1047.
- (4) Johansson, G. *Adv. Inorg. Chem.* **1992**, *39*, 159.
- (5) Sandström, M.; Persson, I.; Ahrlund, S. *Acta Chem. Scand., Ser. A* **1978**, *32*, 607.
- (6) Kepert, D. L.; Taylor, D.; White, A. H. *J. Chem. Soc., Dalton Trans.* **1973**, 670.
- (7) Åkesson, R.; Sandström, M.; Stålhandske, C.; Persson, I. *Acta Chem. Scand.* **1991**, *45*, 165.
- (8) (a) Chudinova, L. I. *Russ. J. Inorg. Chem.* **1969**, *14*, 1568. (b) *Appl. Chem.* **1969**, *42*, 161.
- (9) Inada, Y.; Sugimoto, K.; Ozutsumi, K.; Funahashi, S. *J. Am. Chem. Soc.* **1994**, *33*, 1875.

(10) Persson, I. *J. Coord. Chem.* **1994**, *32*, 261.

(11) Coucouvanis, D. *Prog. Inorg. Chem.* **1979**, *26*, 301.

(12) Wright, J. G.; Natan, M. J.; MacDonnell, F. M.; Ralston, D. M.; O'Halloran, T. V. *Prog. Inorg. Chem., Bioinorg. Chem.* **1990**, *38*, 323.

(13) Strömberg, D.; Sandström, M.; Wahlgren, U. *Chem. Phys. Lett.* **1990**, *172*, 49.

(14) Riddick, J. A.; Bunger, J. W. *Techniques of Chemistry, Organic Solvents*; Wiley-Interscience: New York, 1970.

(15) Diggle, J. W.; Bogsányi, D. *J. Phys. Chem.* **1974**, *78*, 1018.

(16) Stålhandske, C. M. V.; Stålhandske, C. I.; Sandström, M.; Persson, I. *Inorg. Chem.* **1997**, *36*, 3167.

**Table 1.** Composition of the *N,N*-Dimethylthioformamide (DMTF) Solutions Studied by LAXS<sup>a</sup>

	M <sup>2+</sup>	CF <sub>3</sub> SO <sub>3</sub> <sup>-</sup>	ClO <sub>4</sub> <sup>-</sup>	DMTF	V/Å <sup>3</sup>	ρ/g·cm <sup>-3</sup>	μ/cm <sup>-1</sup>
Zn <sup>2+</sup>	0.85	1.70		10.22	2102	1.22	7.42
Cd <sup>2+</sup>	0.86	1.72		10.22	1934	1.26	6.97
Hg <sup>2+</sup>	1.00		2.00	11.21	1677	1.40	39.6

<sup>a</sup> The concentrations in mol·dm<sup>-3</sup>, the stoichiometric unit of volume per metal atom, *V*, the density, *ρ*, at 25 °C, and the linear absorption coefficient, *μ*, for Mo Kα radiation are given.

(see below) and lattice energies for different packing arrangements can easily distort the ideal coordination geometry for a free complex, as is evident from the two crystal structures of cadmium solvates in the preceding article.<sup>16</sup>

A transfer thermodynamic study showed the solvation of the zinc, cadmium, and mercury(II) ions to be much stronger in *N,N*-dimethylthioformamide than in water.<sup>17</sup> The heat of transfer from water to *N,N*-dimethylthioformamide is strongly exothermic for all the divalent group 12 metal ions, consistent with a more pronounced covalent contribution to the metal–solvate bond than in the hydrates, as expected for a strong electron-pair donor. The entropies of transfer are small and suggest a high degree of order in the *N,N*-dimethylthioformamide solvent. Negative values are obtained for zinc but positive for cadmium, which may indicate a different ligand configuration around the two ions.<sup>17</sup> A recent large-angle X-ray scattering study gives further evidence of bulk order in liquid *N,N*-dimethylthioformamide, with features in the radial distribution function consistent with weak intermolecular hydrogen bonding.<sup>18</sup> Also a crystal structure of *N,N*-dimethylthioformamide at low temperature shows weak hydrogen bonds between –CHS hydrogen and sulfur atoms connecting neighboring molecules in zigzag chains.<sup>18</sup> Weak hydrogen bonding is also found in the crystalline *N,N*-dimethylthioformamide solvates of zinc, cadmium, and mercury(II) mentioned above and is discussed in the preceding article.<sup>16</sup> The hexasolvated cadmium ion shows internal C–H···S hydrogen bonding between its *N,N*-dimethylthioformamide ligands, while in the other solvates weak hydrogen bonds can be found between a –CHS hydrogen and an anion oxygen atom.

In order to obtain further information about the bonding and coordination geometry of the solvated zinc, cadmium, and mercury(II) ions with a strongly coordinating monodentate sulfur donor ligand, their structures in *N,N*-dimethylthioformamide solution have been studied in the present work by means of large-angle X-ray scattering, LAXS, and vibrational spectroscopy.

## Experimental Section

**Preparations.** *N,N*-Dimethylthioformamide and the anhydrous trifluoromethanesulfonate salts of zinc and cadmium were synthesized as described previously.<sup>16,19,20</sup> Crystalline solvates were obtained by cooling *N,N*-dimethylthioformamide solutions saturated at 40 °C<sup>16</sup> and used to prepare the zinc and cadmium solutions studied by LAXS; see Table 1.

Crystalline *N,N*-dimethylthioformamide solvates of cadmium and mercury(II) perchlorate were prepared as described previously.<sup>16</sup> The bis(*N,N*-dimethylthioformamide)mercury(II) perchlorate was used to

prepare the solution studied by LAXS, since anhydrous mercury(II) trifluoromethanesulfonate decomposes and forms a black precipitate when added to *N,N*-dimethylthioformamide.

**Warning!** Caution should be exercised when handling organic solvates and solutions of heavy metal perchlorates because of the risk of explosions. When small quantities of bis(*N,N*-dimethylthioformamide)mercury(II) perchlorate were exposed to the intense green laser light in the Raman spectrometer, explosions occurred after some time.

**Large-Angle X-ray Scattering Measurements.** The free surface of saturated zinc and cadmium trifluoromethanesulfonate solutions, 0.85 and 0.86 M, respectively, and a 1.00 M mercury(II) perchlorate solution in *N,N*-dimethylthioformamide were irradiated by Mo Kα X-rays, *λ* = 0.7107 Å, and the scattering was measured by means of a large-angle *θ*–*θ* goniometer, described previously.<sup>21</sup> The intensity data were collected in step scan mode with an interval  $\Delta\theta$  of 0.1° for 1° < *θ* < 25° and 0.25° for 25° < *θ* < 65°. The reflections from a gold plate were used to calibrate the scattering angle *θ* of the goniometer. A vertical Soller slit followed by a horizontal 1° divergence slit was used to limit the primary beam from the X-ray tube, except for small scattering angles (*θ* < 10°) where smaller slits, 1/12 and 1/4°, were necessary. Bragg–Brentano semifocusing geometry was used with a distance between the line focus and sample center of 16.5 cm. After the sample, a scatter slit with twice the size of the divergence slit was followed by a 0.2 mm focal slit (0.1 mm for the 1/12 and 1/4° divergence slits). A focusing LiF monochromator<sup>22</sup> of Johansson type was used to eliminate fluorescence and to partially discriminate against the Compton scattering from the sample. The scattered intensity was recorded by means of a scintillation counter, with further energy discrimination against background radiation and electronic noise obtained by selecting an appropriate energy range on a PC-based multichannel scaling board,<sup>23</sup> reducing the background count rate to about 0.5 cps. At least two scans were made with 10<sup>5</sup> counts collected for each goniometer step, corresponding to a statistical uncertainty of less than 0.3%. The composition, density, and absorption coefficient of the solutions studied are given in Table 1.

**Vibrational Spectra.** The far-IR spectra, 50–500 cm<sup>-1</sup>, were recorded at room temperature by means of a Perkin-Elmer 1760X spectrometer, equipped with a deuterated triglycine sulfate, DTGS, detector. The solid compounds were contained in a polyethylene matrix. For the solutions contained in a cell with silicon windows and a 0.012 mm spacer, 10 000 scans were collected and averaged.

The Raman spectra were excited at ambient temperature with a Coherent Radiation Laboratoires Innova 90-5 argon ion laser using the green line at 514.5 nm with an effective power of about 500 mW at the sample. A DILOR Z24 triple monochromator equipped with a photon counter was used to record digital spectra in the ranges 100–600 cm<sup>-1</sup> and 900–1050 cm<sup>-1</sup> with a spectral bandwidth of 4 cm<sup>-1</sup>. The band positions are estimated to be accurate within ±1 cm<sup>-1</sup> from calibration measurements.

**Treatment of LAXS Data.** Absorption corrections of the measured intensities for the zinc and cadmium solutions were necessary because of the relatively low absorption, Table 1, and applied on each slit combination.<sup>24</sup> The experimental intensities from different scans were scaled to a common basis, corrected for polarization, and normalized to a stoichiometric unit of volume corresponding to one metal atom, as previously described.<sup>21,25</sup> The reduced structure-dependent intensities *i*(*s*) were obtained after subtraction of the sum of the calculated structure-independent scattering.<sup>26</sup> The incoherent part, *i.e.* the Compton scattering,<sup>26</sup> was corrected for recoil effects in the form appropriate for a scintillation counter<sup>27</sup> and multiplied by an instrumental function describing the fraction passing through the LiF monochromator (ca. 0.06 for *s* > 10 Å<sup>-1</sup>). The coherent part of the structure-independent

- (17) Chaudhry, M.; Dash, K. C.; Kinjo, Y.; Persson, I. *J. Chem. Soc., Faraday Trans.* **1994**, *90*, 2235.  
 (18) Stålhandske, C. M. V.; Borrman, H.; Persson, I.; Sandström, M. Unpublished results. See: Stålhandske, C. M. V. Ph.D. Thesis, Swedish University of Agricultural Sciences, Uppsala, 1996.  
 (19) Gutmann, V.; Danksagmüller, K.; Duschek, O. *Z. Phys. Chem., Neue Folge (Frankfurt)* **1974**, *92*, 199.  
 (20) Hedwig, G. R.; Parker, A. J. *J. Am. Chem. Soc.* **1974**, *96*, 6589.

- (21) Johansson, G. *Acta Chem. Scand.* **1966**, *20*, 553; **1971**, *25*, 2787.  
 (22) Crimatec, B. P. 521, 77794 Nemours, Cédex, France.  
 (23) AccuSpec FMS Masterboard, Canberra, Nuclear Data Systems, Golf and Meacham Roads, Schaumburg, IL 60196.  
 (24) Milberg, M. *J. Appl. Phys.* **1958**, *29*, 64.  
 (25) Johansson, G.; Sandström, M. *Chem. Scr.* **1973**, *4*, 195.  
 (26) (a) Cromer, D. T.; Mann, J. B. *J. Chem. Phys.* **1967**, *47*, 1892. (b) Cromer, D. T. *Ibid.* **1969**, *50*, 4857.  
 (27) Dwiggins, C. W., Jr.; Park, D. A. *Acta Crystallogr., Sect. A* **1971**, *27*, 264.

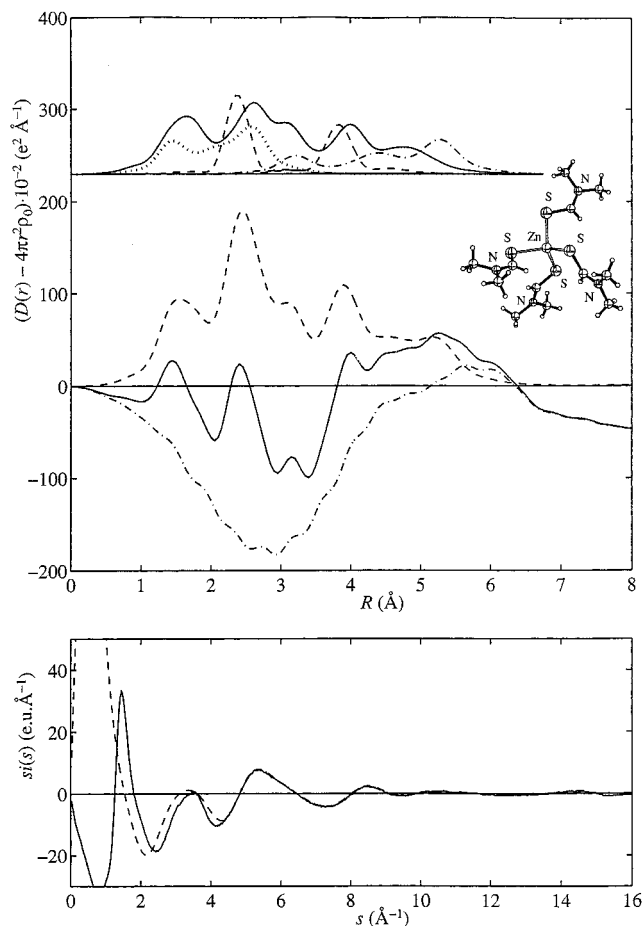


**Figure 1.** LAXS radial distribution curves for 0.85 M zinc trifluoromethanesulfonate in *N,N*-dimethylthioformamide. (Top) Separate model contributions: Zn–S, S···S (dashes), Zn···C, Zn···N (dash-dots) from the complex (see insert); CF<sub>3</sub>SO<sub>3</sub><sup>−</sup> ion (dots); solvent molecules (solid line). (Middle) Experimental  $D(r) - 4\pi r^2 \rho_0$  (solid line); model (dots); difference (dash-dots). (Bottom) Reduced LAXS intensity functions  $s \cdot i(s)$  (solid line); model  $s \cdot i_{\text{calc}}(s)$  (dots).

scattering<sup>25</sup> was calculated using scattering factors,  $f(s)$ , for the neutral atoms, including their anomalous dispersion corrections,  $\Delta f'$  and  $\Delta f''$ .<sup>28</sup> The scattering variable is  $s = (4\pi \sin \theta)/\lambda$ . A Fourier transformation of the reduced intensity function is performed by means of the KURVLR program to give a modified radial distribution function (RDF) according to the expression

$$D(r) - 4\pi r^2 \rho_0 = (2r/\pi) \int_{s_{\min}}^{s_{\max}} s \cdot i(s) M(s) \sin(rs) ds$$

where  $M(s)$  is a modification function and  $\rho_0$  the average scattering density.<sup>25</sup>

Model contributions to the reduced intensities,  $i_{\text{calc}}(s)$ , from well-defined atomic pair interactions between the atoms  $p$  and  $q$  within the proposed molecular models were calculated by means of the following formula:<sup>25</sup>

$$i_{\text{calc}}(s) = [f_p(s)f_q(s) + \Delta f''_p \Delta f''_q] (\sin s d_{pq}) (s d_{pq})^{-1} \exp(-1/2 l_{pq}^2 s^2)$$

The exponent of the Debye–Waller factor contains the mean-square variation  $l_{pq}^2$  of the interatomic distance  $d_{pq}$  assuming a Gaussian distribution of the displacement in  $r$ -space.

A Fourier-transformation of  $i_{\text{calc}}(s)$  was performed in the same way as described above, to obtain peak shapes corresponding to distinct interatomic distances.<sup>25</sup> These peak shapes represent the contributions

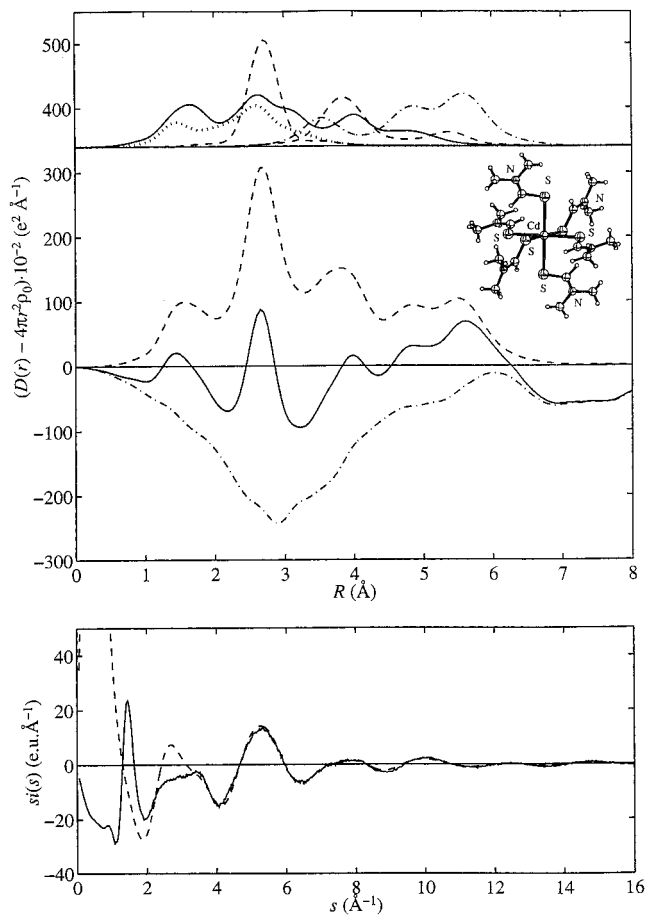


**Figure 2.** LAXS radial distribution curves for 0.86 M cadmium trifluoromethanesulfonate in *N,N*-dimethylthioformamide. (Top) Separate model contributions: Cd–S, S···S (dashes), Cd···C, Cd···N (dash-dots) from complex (see insert); CF<sub>3</sub>SO<sub>3</sub><sup>−</sup> ion (dots); solvent molecules (solid line). (Middle) Experimental  $D(r) - 4\pi r^2 \rho_0$  (solid line); model (dots); difference (dash-dots). (Bottom) Reduced LAXS intensity functions  $s \cdot i(s)$  (solid line); model  $s \cdot i_{\text{calc}}(s)$  (dots).

to the RDF from distances within the complexes and molecules, and when all intramolecular model peak shapes are subtracted, a smooth difference function in  $r$ -space should remain from the diffuse intermolecular interactions of the solution structure.

Diffuse and long-range interatomic interactions give contributions to the  $i(s)$  function which are rapidly damped out for increasing  $s$  values, and prominent and distinct interactions, in particular bonds between heavy atoms, dominate at high  $s$  values. Therefore, model parameters can be adjusted in this region by a least-squares fitting of weighted  $i_{\text{calc}}(s)$  and experimentally derived  $i(s)$  values, in a similar way as is normal for data from EXAFS, extended X-ray absorption fine structure spectroscopy. However, for the LAXS data the fit of this type of model representing the coordinated distances in the solution should be evaluated not only from the intensity functions above a lower limit in  $s$ -space but also from the Fourier-transformed difference function in  $r$ -space.

For the present models, which do not include diffuse intermolecular interactions, least-squares refinements of model parameters minimizing the error square sum  $U = \sum s^2 [i_{\text{exp}}(s) - i_{\text{calc}}(s)]^2$  were performed with the use of the STEPLR program above a lower limit of  $s > 4 \text{ \AA}^{-1}$ ; cf. Figures 1–3.<sup>30</sup> Prior to the refinements minor spurious peaks below  $1.2 \text{ \AA}$  in the radial distribution functions which could not be related to interatomic distances were eliminated by a Fourier back-transform procedure.<sup>31</sup> The effect is to remove corresponding low-frequency

(28) *International Tables for Crystallography*; Wilson, A. J. C., Ed.; Kluwer Academic Publishers: Dordrecht, The Netherlands, 1995; Vol. C.

(29) Sandström, M.; Johansson, G. *Acta Chem. Scand., Ser. A* **1977**, *31*, 132.

(30) Molund, M.; Persson, I. *Chem. Scr.* **1985**, *25*, 197.

(31) Levy, H. A.; Danford, M. D.; Narten, A. H. *Data Collection and Evaluation with X-ray Diffractometer Designed for the Study of Liquid Structure*; Technical Report ORNL-3960; Oak Ridge National Laboratory: Oak Ridge, TN, 1966.

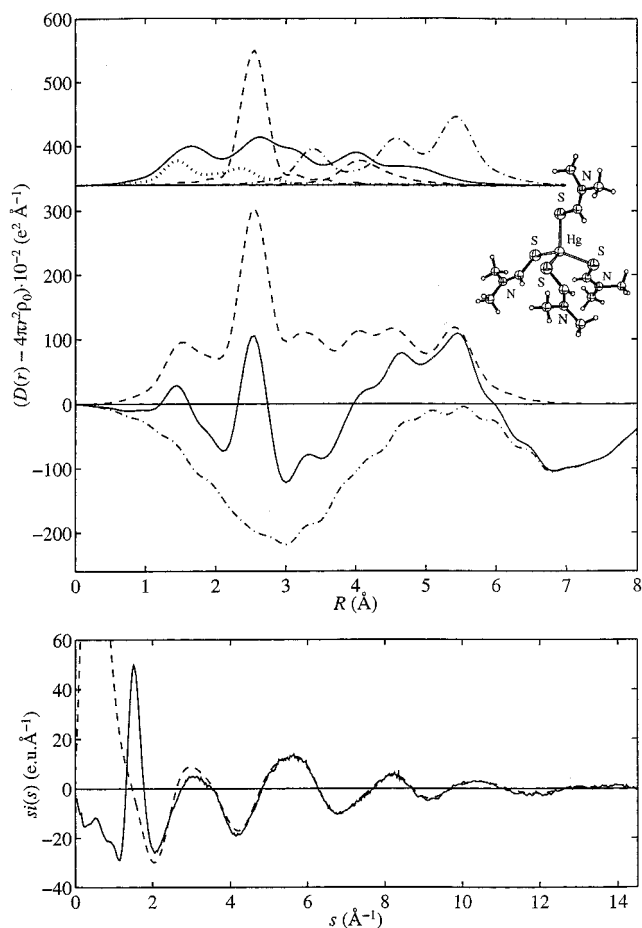


**Figure 3.** LAXS radial distribution curves for 1.00 M mercury(II) perchlorate in *N,N*-dimethylthioformamide. (Top) Separate model contributions: Hg–S, S···S (dashes), Hg···C, Hg···N (dash-dots) from complex (see insert); ClO<sub>4</sub><sup>−</sup> ion (dots); solvent molecules (solid line). (Middle) Experimental  $D(r) - 4\pi r^2 \rho_0$  (solid line); model (dots); difference (dash-dots). (Bottom) Reduced LAXS intensity functions  $s \cdot i(s)$  (solid line); model  $s \cdot i_{\text{calc}}(s)$  (dots).

oscillations of the experimental  $i(s)$  function to obtain a better alignment along the  $s$ -axis.

The models used include the atomic pair interactions between the metal ion and the ligand atoms and also the S···S distances within the solvated metal ions and the intramolecular distances of the *N,N*-dimethylthioformamide molecule and of the anions. There is in general a strong correlation between the number  $n$  of interatomic distances  $d_{pq}$  and the corresponding displacement parameter  $l_{pq}$ . Therefore, different calculations were made with the coordination number of the complexes fixed at the possible integer values and with initial parameter values for each atomic pair interaction obtained from comparison with crystal structures and previous LAXS investigations.<sup>16,18</sup> Some distances and displacement parameters of the complexes were then varied to improve the fit, while the parameters of several well-known and/or minor interactions were kept constant. The perchlorate ion is described in tetrahedral geometry with the Cl–O distance 1.425 Å<sup>32</sup> and the trifluoromethanesulfonate ion as in crystal structures with the main distances C–F 1.336 Å and S–O 1.442 Å.<sup>33</sup> The fit between calculated and experimental data improved markedly when also intermolecular distances corresponding to about 50% hydrogen bonding between the free *N,N*-dimethylthioformamide molecules were introduced in a similar way as for the pure solvent.<sup>18</sup> The parameters used describe the hydrogen bond S···C distance of 3.86 Å with the displacement parameter  $l = 0.10$  Å and intermolecular S···S and S···C distances of

**Table 2.** Model Parameters for the Solvated Metal Ion Complexes  $[M(\text{SCHN}(\text{CH}_3)_2)_n]^{2+}$  Used in the LAXS Calculations<sup>a</sup>

	dist	Zn	Cd	Hg
M–S	$d$	2.362(5)	2.69(1)	2.527(6)
	$l$	0.095(6)	0.16(1)	0.10(1)
	$n$	4	6	4
M–C	$d$	3.19(5)	3.52 <sup>b</sup>	3.37(5)
	$l$	0.17(4)	0.17	0.14(4)
	$n$	4	6	4
S···S <sub>comp</sub>	$d$	3.83(3)	3.70/3.97 <sup>b</sup>	4.03(6)/4.2 <sup>c</sup>
	$l$	0.12(2)	0.20	0.18(6)/0.1 <sup>c</sup>
	$n$	6	6/6 <sup>d</sup>	5/1 <sup>d</sup>
M–N	$d$	4.35(6)	4.79(4)	4.55(3)
	$l$	0.24(3)	0.22(3)	0.17(5)
	$n$	4	6	4
M–C'	$d$	5.25	5.59	5.43
	$l$	0.28	0.25	0.17
	$n$	8	12	8
M–S–C/deg		103(2) <sup>e</sup>		105(3) <sup>e</sup>

<sup>a</sup> Distance  $d/\text{Å}$ , displacement parameter  $l/\text{Å}$ , and number of distances/metal atom  $n$ . S···S<sub>comp</sub> is the sulfur–sulfur distance within the complex. For parameters refined by least-squares methods probable errors are given (within brackets, 90% confidence limit). <sup>b</sup> From crystal structure.<sup>16</sup> <sup>c</sup> Estimated; see text. <sup>d</sup> Number of interactions for each S···S distance. <sup>e</sup> Calculated assuming S–C 1.68 Å.<sup>16</sup>

4.85 and 4.20 Å with  $l = 0.30$  and 0.26 Å, respectively, between neighboring *N,N*-dimethylthioformamide molecules.<sup>18</sup>

The model functions for the coordination numbers which gave the best fits to the experimental data are shown in Figures 1–3, and the parameters which could be refined are given with their estimated standard errors in Table 2. The uncertainty in the coordination numbers is estimated to  $\pm 0.5$ . Least-squares refinements were made in different  $s$ -ranges in order to detect possible angle-dependent errors in the intensity data.

## Results and Discussion

**Large-Angle X-ray Scattering.** The experimental radial distribution function, RDF, of the zinc solution in *N,N*-dimethylthioformamide and the model function including separate contributions from different entities in the model are shown in Figure 1. The Zn–S and S···S distances from the solvated zinc ion give major contributions to the distinct peaks at 2.4 and 3.8 Å; the corresponding distances in the solid  $[\text{Zn}(\text{SCHN}(\text{CH}_3)_2)_4](\text{CF}_3\text{SO}_3)_2$  compound are 2.35 Å (corrected for riding motion) and 3.83 Å, respectively.<sup>16</sup> All four peaks in the RDF at about 1.5, 2.4, 3.2, and 3.8 Å correspond to intramolecular distances within the *N,N*-dimethylthioformamide molecule and the trifluoromethanesulfonate ion.<sup>16,18</sup> Despite the overlap, some contributions from the complex, in particular Zn–S, are sufficiently distinct to allow least-squares refinements of their model parameters (see above), which gave Zn–S and S···S distances of 2.362(5) and 3.83(3) Å, respectively, Table 2. The ratio 0.617(6) between these distances is close to the value 0.612 expected for a regular tetrahedral arrangement and shows that the  $[\text{Zn}(\text{SCHN}(\text{CH}_3)_2)_4]^{2+}$  complexes are similar in solution and in the solid state.

The peak at 1.5 Å in the RDF of the cadmium solution, cf. Figure 2, originates from the same type of intramolecular distances as for the zinc solution. The major peak at 2.7 Å is dominated by the Cd–S interactions but in addition contains contributions from intramolecular distances within the solvent molecules and the anion. The next broad peak at 3.8 Å results from the S···S distances within the complex with some contribution from the *N,N*-dimethylthioformamide molecules. In the crystal structure of  $[\text{Cd}(\text{SCHN}(\text{CH}_3)_2)_6](\text{ClO}_4)_2$  the mean Cd–S bond length is 2.715 Å, slightly longer than the solution value 2.69(1) Å obtained by a least-squares refinement of a six-

(32) Berglund, B.; Thomas, J. O.; Tellgren, R. *Acta Crystallogr., Sect. B* **1975**, *31*, 1842.

(33) Nieuwpoort, G.; Verschoor, G.; Reedijk, J. *J. Chem. Soc., Dalton Trans.* **1983**, 531.

coordinated complex, Table 2. Attempts to refine a single S...S distance, assuming a Gaussian distribution described by a Debye–Waller type of displacement parameter, resulted in an unusually large spread around the mean value which then also partially overlapped and affected the Cd...C distance of the model, expected at 3.52 Å from the crystal structure.<sup>16</sup> However, S...S distances shorter than van der Waals contacts (about  $2 \times 1.8 \text{ Å}$ )<sup>12</sup> are unlikely to occur. Moreover, the S...S distances of the slightly distorted centrosymmetric Cd(SCHN(CH<sub>3</sub>)<sub>2</sub>)<sub>6</sub><sup>2+</sup> complex in the crystal structure fall into two distinct groups (within  $\pm 0.03 \text{ Å}$  in each) with mean values 3.70 and 3.97 Å.<sup>16</sup> Therefore, the S...S and the Cd–C distances were held fixed at the mean crystal structure values in the final refinements of the model, which gave a satisfactory fit to the experimental data, Figure 2.

When the saturated solution of cadmium trifluoromethanesulfonate investigated by LAXS crystallizes, the solid phase comprises [Cd(SCHN(CH<sub>3</sub>)<sub>2</sub>)<sub>4</sub>(O<sub>3</sub>SCF<sub>3</sub>)<sub>2</sub>] complexes in which the cadmium atom is octahedrally surrounded by four sulfur and two oxygen atoms at 2.65 and 2.47 Å, respectively.<sup>16</sup> However, no such direct interactions to the trifluoromethanesulfonate ions can be detected in the RDF of this solution, nor was there any indication of tetrahedral coordination, which is common in complexes with bridging S-ligands and should have given Cd–S and S...S distances of about 2.5 and 4.1 Å, respectively.<sup>34</sup> With the bidentate ligand cyclohexyl thioxanthate cadmium forms another six-coordinated sulfur complex with Cd–S distances in the range 2.668–2.721 Å,<sup>34</sup> close to the present solution value.

The peak at 1.5 Å in the RDF of the mercury(II) solution, cf. Figure 3, has contributions from the perchlorate ion, Cl–O 1.43 Å, and the *N,N*-dimethylthioformamide molecule. The peak at about 2.5 Å is strongly dominated by the Hg–S distance but also includes contributions from intramolecular distances in the *N,N*-dimethylthioformamide molecule and from the tetrahedral perchlorate ion with O...O 2.34 Å. In the solid bis-solvate [Hg(SCHN(CH<sub>3</sub>)<sub>2</sub>)<sub>2</sub>](ClO<sub>4</sub>)<sub>2</sub> two collinear Hg–S bonds are found with a much shorter distance, 2.354 Å.<sup>16</sup> However, metacinnabarite with tetrahedral coordination has an Hg–S bond length of 2.543 Å,<sup>35</sup> close to the present solution value which is refined to 2.527(6) Å (Table 2). The S...S distance for a regular tetrahedral Hg–S coordination would then be expected at 4.13 ( $2.527\sqrt{8/3}$ ) Å. The best fit is obtained for a mean S...S distance of 4.03(6) Å, which indicates some distortion of a tetrahedral geometry. Another distorted tetrahedron of sulfur atoms around the mercury atom is found in tetrakis(thiourea)-mercury(II) chloride where one long Hg–S' distance was found to give smaller than tetrahedral S'–Hg–S angles.<sup>36</sup> The  $\alpha$ -form of mercury(II) *N,N*-diethyldithiocarbamate has a highly distorted tetrahedral Hg–S coordination with one Hg–S bond much shorter, 2.418(7) Å, than the mean at 2.57 Å. Also this type of deformation leads to a group of S...S distances with a shorter average value than that expected for a regular tetrahedral structure.<sup>37</sup> The mean S...S distance 4.03 Å obtained for the Hg(SCHN(CH<sub>3</sub>)<sub>2</sub>)<sub>4</sub><sup>2+</sup> complex in solution is consistent with a similar, although possibly smaller, distortion since no splitting of the Hg–S distances could be discerned. The displacement parameter of the Hg–S distance (Table 2) corresponds to a root-mean-square variation of  $l = 0.10 \text{ Å}$  and is only slightly larger

than that found in a LAXS study of the Hg(SCN)<sub>4</sub><sup>2-</sup> complex in dimethyl sulfoxide solution.<sup>38</sup>

The small peak at about 3.3 Å can be attributed to the closest Hg...C distance of the solvated ion. The refined Hg–S and Hg...C distances (Table 2) give a mean Hg–S–C angle of 105–(3)° for an S–C bond distance of 1.68 Å.<sup>16</sup> The separate contributions for the main atomic pair interactions of the model are shown in Figure 3.

In all the solid solvates the metal ions are close to the plane of the *N,N*-dimethylthioformamide ligands, and the M–S–C angles fall in the range 101–107°.<sup>16</sup> This results in two almost equal metal ion–methyl carbon (C') distances for each ligand. The mean M...C' distance is also observable in the RDFs of all three solutions with distinguishable peaks at 5.3, 5.6, and 5.43 Å for zinc, cadmium, and mercury, respectively (Figures 1–3). The mean M...C' distances for the solid four- and six-coordinated zinc and cadmium solvates are 5.34 and 5.69 Å, respectively.<sup>16</sup> The slightly shorter M...C' distances in solution than in the solid compounds may well be caused by a larger out-of-plane bending of the ligands due to interaction or ion-pair formation between the solvated metal ions and the anions in these concentrated electrolyte solutions; see further discussion below. The mean M...C', M...N, and M...C distances used in the fitting of model interactions to the RDFs (Table 2) correspond to the known geometry of the planar *N,N*-dimethylthioformamide ligands.

It is obvious that the change from six-coordination for the solvated cadmium ion to four-coordination for the mercury(II) ion in *N,N*-dimethylthioformamide cannot be caused by steric hindrance, as the cadmium ion is the smaller one. Generally, the difference is at least 0.05 Å between the mean M–O bond distances in comparable six-coordinated solvates of cadmium and mercury(II) ions, e.g. with water and dimethyl sulfoxide.<sup>5,39</sup> The zinc ion is six-coordinated in the oxygen or nitrogen donor solvents water,<sup>4</sup> dimethyl sulfoxide<sup>5</sup> and pyridine,<sup>8</sup> whereas the coordination number is 4 in the more strongly electron-pair donating solvents *N,N*-dimethylthioformamide and liquid ammonia.<sup>40,41</sup> This clearly shows a connection between the decrease in coordination number and the properties of the metal ion–solvate bonds, both for the zinc and mercury(II) ions.

In tetrakis(*N,N*-dimethylthioformamide)zinc trifluoromethanesulfonate, the average Zn–S bond distance 2.34 Å (2.35 Å after a riding motion correction)<sup>16</sup> is close to the Zn–S bond distance in zinc sulfide, 2.342 Å.<sup>42</sup> A slightly but not significantly longer Zn–S bond distance is obtained for the *N,N*-dimethylthioformamide solution, 2.362(5) Å, Table 2. However, the six-coordinated cadmium complex has a slightly shorter mean Cd–S bond distance in solution, 2.69(1) Å, than in the solid state, 2.715 Å.<sup>16</sup> The same tendency is also found for the six-coordinated solvates of iron(II) with *N,N*-dimethylthioformamide. The Fe–S bond distance in solution, 2.52(1) Å, determined by EXAFS,<sup>43</sup> is slightly shorter than the mean value from a crystal structure determination of hexakis(*N,N*-dimethylthioformamide)iron(II) perchlorate, 2.54 Å.<sup>44</sup> Normally, bond lengths obtained from single-crystal diffraction studies appear to be slightly shorter than corresponding solution values by EXAFS or LAXS methods because of the different influence

(34) Sola, J.; Gonzalez-Duarte, P.; Sanz, J.; Casals, I.; Alsina, T.; Sobrados, I.; Alvarez-Larena, A.; Piniella, J. F.; Solans, X. *J. Am. Chem. Soc.* **1993**, *115*, 10018.

(35) Aurivillius, K. *Acta Chem. Scand., Ser. A* **1964**, *18*, 1552.

(36) Brotherton, P. D.; White, A. H. *J. Chem. Soc., Dalton Trans.* **1973**, 2696.

(37) Iwasaki, H. *Acta Crystallogr., Sect. B* **1973**, *29*, 2115.

(38) Iverfeldt, Å.; Persson, I.; Åhrland, S. *Acta Chem. Scand., Ser. A* **1981**, *35*, 295.

(39) Johansson, G.; Sandström, M. *Acta Chem. Scand., Ser. A* **1987**, *41*, 113.

(40) Schmidt, K. H.; Müller, A. *Coord. Chem. Rev.* **1976**, *19*.

(41) Gans, P.; Gill, B. *J. Chem. Soc., Dalton Trans.* **1976**, 779.

(42) Yamanaka, T.; Tokonami, M. *Acta Crystallogr., Sect. B* **1985**, *41*, 298.

(43) Persson, I. Unpublished results.

(44) Baumgartner, O. *Acta Crystallogr., Sect. C* **1986**, *42*, 1723.

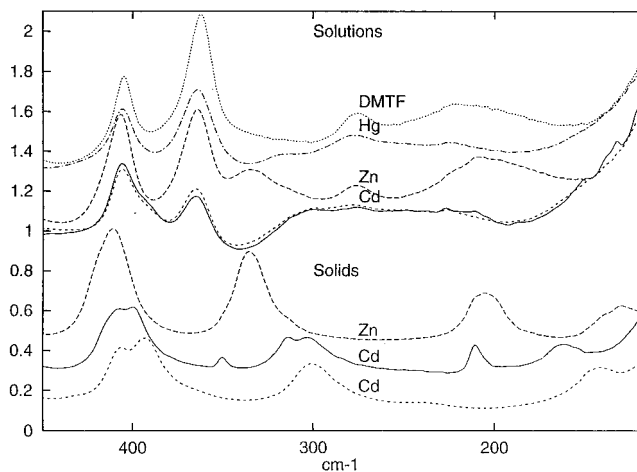


**Figure 4.** Far-IR spectra 120–450  $\text{cm}^{-1}$  of the solvated zinc, cadmium, and mercury(II) ions and of *N,N*-dimethylthioformamide (dots). The anions are  $\text{CF}_3\text{SO}_3^-$  for zinc (dashes) and cadmium (solid line), and  $\text{ClO}_4^-$  for mercury (dash-dots) and cadmium (small dashes).

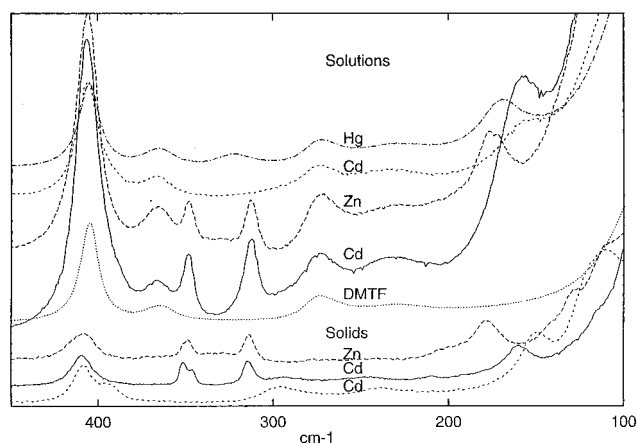


**Figure 5.** Raman spectra 100–450  $\text{cm}^{-1}$  of the solvated zinc, cadmium, and mercury(II) ions and of pure *N,N*-dimethylthioformamide (dots). The anions are  $\text{CF}_3\text{SO}_3^-$  for zinc (dashes) and cadmium (solid line), and  $\text{ClO}_4^-$  for mercury (dash-dots) and cadmium (small dashes).

from thermal motion.<sup>16,45</sup> The unexpected opposite trend observed here for the cadmium and iron(II) complexes is probably due to the internal hydrogen bonds formed between the *N,N*-dimethylthioformamide ligands within these solid hexasolvates, weakening the metal–sulfur bonds as discussed in the preceding article.<sup>16</sup> No hydrogen bonding was found between the ligands of the tetrahedral  $[\text{Zn}(\text{SCHN}(\text{CH}_3)_2)_4]^{2+}$  complex in the crystal structure.<sup>16</sup>

Broad but prominent features can be seen in the RDFs at about 9–10 Å, cf. Figures 1–3, and also at 14 Å. Because of the high metal ion concentration in the studied solutions (Table 1) only a few, 5–7, free *N,N*-dimethylthioformamide molecules will remain between the solvated complexes together with the anions. The solutions can thus be expected to show similarities to a solvated melt with some regularity of the medium-range distances due to an organized packing of the charged species.

**Vibrational Spectroscopy.** Far-IR and Raman spectra of the solutions and also of the solid solvates are shown in Figures 4 and 5, and the vibrational frequencies with the proposed assignments are summarized in Table 3. The bands obtained can be divided into three groups of origin, the internal vibrations

of the *N,N*-dimethylthioformamide molecule,<sup>46</sup> the metal ion–solvate bonds, and the trifluoromethanesulfonate or perchlorate anions.<sup>47,48</sup> No significant frequency shifts are found for the anions, as expected for noncoordinated or weakly interacting species.<sup>48</sup> However, for the coordinated *N,N*-dimethylthioformamide molecules some shifts and intensity changes occur. An obvious difference between the spectra of the pure solvent and the solutions is the intensity change of the characteristic *N,N*-dimethylthioformamide IR absorption bands at 363 and 405  $\text{cm}^{-1}$ ; cf. Figure 4. Normal coordinate analyses show that the corresponding normal modes involve the amide part of the *N,N*-dimethylthioformamide molecule.<sup>46</sup> The first is the nitrogen out-of-plane deformation,  $\gamma(\text{C}'\text{N})$ , and the second is the scissoring+rocking deformation mode of the dimethylamino group,  $\sigma(\text{NC}_2') + \rho(\text{NC}_2')$  in Table 3. In pure *N,N*-dimethylthioformamide the IR absorption at 363  $\text{cm}^{-1}$  is the strongest of the two, but its intensity gradually decreases for solutions with decreasing number of free solvent molecules and disappears for the solids, Figure 4. This is consistent with a hindered out-of-plane vibration in the coordinated molecule. The 405  $\text{cm}^{-1}$  deformation mode changes very little for all the complexes (Table 3), except for the solid mercury(II) solvate with very strongly coordinated *N,N*-dimethylthioformamide ligands.

The strongest contribution to the 967  $\text{cm}^{-1}$  band in the *N,N*-dimethylthioformamide spectrum is from C–S stretching. This band shifts toward lower frequency in the complexes as expected for coordination to the sulfur atom. The band at about 276  $\text{cm}^{-1}$  of the *N,N*-dimethylthioformamide molecule is dominated by S–C deformation,  $\delta(\text{CS})$ , with a contribution of amino group rocking  $\rho(\text{NC}_2')$  and a lowering of the frequency is expected at coordination as observed for the solids; cf. Table 3.

Generally, the normal modes involving metal ion–solvate vibrations were found to be strongly coupled with the *N,N*-dimethylthioformamide ligand vibrations. Normal coordinate analysis has been performed on the vibrational spectrum of the linear bis(*N,N*-dimethylthioformamide)mercury(II) complex in the solid perchlorate salt.<sup>46</sup> The asymmetric Hg–S stretching,  $\nu_{\text{as}}(\text{HgS})$ , was found to contribute strongly to the band found at 382  $\text{cm}^{-1}$  but also to the S–C deformation band found at 184  $\text{cm}^{-1}$ . The symmetric S–Hg–S stretching,  $\nu_{\text{s}}(\text{HgS})$ , gives the main contribution to the 360  $\text{cm}^{-1}$  band but also contributes to the S–C bending mode at 191  $\text{cm}^{-1}$ . The linear S–Hg–S in-plane bending,  $\delta_{\text{s}}(\text{HgS}_2)$ , out-of-plane bending  $\delta'_{\text{s}}(\text{HgS}_2)$ , and the Hg–S–C bending,  $\delta_{\text{s}}(\text{HgSC})$ , modes were assigned to the bands at 104, 145, and 115  $\text{cm}^{-1}$ , respectively.

The Raman spectrum of the tetrahedrally coordinated mercury(II) complex in *N,N*-dimethylthioformamide solution shows two polarized low-frequency Raman bands, at 172 and 323  $\text{cm}^{-1}$ . The symmetric Hg–S stretching contributes strongly to both these bands, although with significant coupling in the 172  $\text{cm}^{-1}$  normal mode to skeletal deformations of the *N,N*-dimethylthioformamide ligands, as in the 184 and 191  $\text{cm}^{-1}$  modes in the linear two-coordinated complex (Table 3). The asymmetric S–Hg–S stretching contribution is not as prominent as in the 382  $\text{cm}^{-1}$  band of the linear complex but contributes to the infrared band at 317  $\text{cm}^{-1}$ . S–Hg–S deformation is probably the main contribution to the band at 100  $\text{cm}^{-1}$ .

The assignments for the  $[\text{Zn}(\text{SCHN}(\text{CH}_3)_2)_4]^{2+}$  complex can be aided by comparisons with a simplified normal coordinate analysis of the  $[\text{N}(\text{CH}_3)_4]_2[\text{Zn}(\text{SC}_6\text{H}_5)_4]$  compound, performed

(46) Stålhandske, C. M. V.; Mink, J.; Sandström, M.; Papai, I.; Johansson, P. *Vibr. Spectr.* **1997**, *498*, in press.

(47) Johnston, D. H.; Shriver, D. F. *Inorg. Chem.* **1993**, *32*, 1045.

(48) Nakamoto, K. *Infrared and Raman Spectra of Inorganic and Coordination Compounds*, 4th ed.; Wiley-Interscience: New York, 1986; Chapter II-6.

(45) Trueblood, K. N. In *Accurate Molecular Structures*; IUCr Monographs on Crystallography, No. 1; Domenicano, A., Hargittai, I., Eds.; Oxford University Press: Oxford, U.K., 1992; Chapter 8.

**Table 3.** Far-IR and Raman Spectra ( $\text{cm}^{-1}$ ) for the Solids  $[\text{Zn}(\text{SCHN}(\text{CH}_3)_2)_4](\text{CF}_3\text{SO}_3)_2$ ,  $[\text{Cd}(\text{SCHN}(\text{CH}_3)_2)_4(\text{O}_3\text{SCF}_3)_2]$ ,  $[\text{Cd}(\text{SCHN}(\text{CH}_3)_2)_6](\text{ClO}_4)_2$ , and  $[\text{Hg}(\text{SCHN}(\text{CH}_3)_2)_2](\text{ClO}_4)_2$  and for the Corresponding *N,N*-Dimethylthioformamide Solutions and Pure Solvent<sup>g</sup>

<i>N,N</i> -Dimethylthioformamide $\text{SCHN}(\text{CH}_3)_2$									
IR		Raman		assgnt <sup>a</sup>	IR		Raman		assgnt <sup>a</sup>
191 m				$\tau(\text{NCH}_3)$	405 s		405 m		$\sigma(\text{NC}_2')$ , $\rho(\text{NC}_2')$
220 m		229 vw		$\tau(\text{NCH}_3)$	520 s		522 m		$\sigma(\text{NC}_2')$ , $\delta(\text{CS})$
276 m		273 w		$\delta(\text{CS})$ , $\rho(\text{NC}_2')$	970 s		967 s		$\nu(\text{CS})$
363 vs		365 w		$\gamma(\text{C}'\text{N})$					
$[\text{Zn}(\text{SCHN}(\text{CH}_3)_2)_4](\text{CF}_3\text{SO}_3)_2$									
IR		Raman		assgnt <sup>a</sup>	IR		Raman		assgnt <sup>a</sup>
soln	cryst	soln	cryst		soln	cryst	soln	cryst	
130 m		110 m		$\delta(\text{ZnS}_2)$	335 m 335 s		331 332 vw		$\nu(\text{Zn-S})$
139 m		130 m			364 s		348 w 349 m		$\text{CF}_3\text{SO}_3^-$ : $\rho(\text{SO}_3)^c$
180 vw		175 <sup>b</sup> w		$\delta(\text{CS})$ , $\nu_s(\text{Zn-S})$	407 s 409 s		366 w 366 w		$\gamma(\text{C}'\text{N})$
210 m		178 m			406 m 408 m		406 m 408 m		$\sigma(\text{NC}_2')$ , $\rho(\text{NC}_2')$
221sh		205 w		$\text{CF}_3\text{SO}_3^-$ : $\rho(\text{CF}_3)^c$			521 m 519 m		$\sigma(\text{NC}_2')$ , $\delta(\text{CS})$
276 m		230 vw		$\tau(\text{NCH}_3)$			938 w 940 m		$\nu(\text{CS})^d$
317 w		272 w		$\delta(\text{CS})$ , $\rho(\text{NC}_2')$			968 s 969 m		$\nu(\text{CS})^e$
315 w		312 w		$\text{CF}_3\text{SO}_3^-$ : $\nu_s(\text{CS})^c$					
312 w		313 m							
Cadmium Complexes									
$[\text{Cd}(\text{SCHN}(\text{CH}_3)_2)_4(\text{O}_3\text{SCF}_3)_2]$					$[\text{Cd}(\text{SCHN}(\text{CH}_3)_2)_6](\text{ClO}_4)_2$				
IR		Raman		assgnt <sup>a</sup>	IR		Raman		assgnt <sup>a</sup>
soln	cryst	soln	cryst		soln	cryst	soln	cryst	
132 m		118 s		117 w	142 m		155 <sup>b</sup> m 148 s		$\delta(\text{CS})$ , $\delta_s(\text{CdS})$
211 w		161 m		149 m	238 w		232 w 238 w		$\text{CF}_3\text{SO}_3^-$ : $\rho(\text{CF}_3)^c$
227m		230 vw		227 w	273 w		273 w 295 w		$\tau(\text{NCH}_3)$
249 w		234 vw		249 w	301 m		293 vw 295 w		$\delta(\text{CS})$ , $\rho(\text{NC}_2')$
276 m		242 vw		279 w	366 w		366 w 394 w		$\nu_s(\text{Cd-S})$
299 m		250 vw		298 w	390 vw		390 vw 394 w		$\text{CF}_3\text{SO}_3^-$ : $\nu_s(\text{CS})^c$
313 w		273 vw		301 m	405 m		405 m 408 m		$\text{CF}_3\text{SO}_3^-$ : $\rho(\text{SO}_3)^d$
365 m		303 m		365 m	460 w		458 m 459 w		$\text{CF}_3\text{SO}_3^-$ : $\rho(\text{SO}_3)^c$
394 m		314 m		393 m	461 m		458 m 459 w		$\gamma(\text{C}'\text{N})$
408 s		350 m		408 s	520 m		520 m 520 s		$\nu_{\text{as}}(\text{Cd-S})$ , $\rho(\text{NC}_2')$
		365 w		409 m	520 m		520 m 520 s		$\sigma(\text{NC}_2')$ , $\rho(\text{NC}_2')$
		390 w		460 w	520 m		520 m 520 s		$\delta(\text{ClO}_4)^f$
		406 m		520 m	951 m		951 m 949 s		$\sigma(\text{NC}_2')$ , $\delta(\text{CS})$
		409 m		520 m	967 s		967 s 968 <sup>d</sup> w		$\nu(\text{CS})^d$
		520 m		520 m					$\nu(\text{CS})^e$
		520 m		520 m					
		951 m		951 m					
		968 s		968 <sup>d</sup> w					
Mercury Complexes									
$[\text{Hg}(\text{SCHN}(\text{CH}_3)_2)_2](\text{ClO}_4)_2$				$[\text{Hg}(\text{SCHN}(\text{CH}_3)_2)_4](\text{ClO}_4)_2$					
IR cryst		Raman cryst		assgnt	IR soln		Raman soln		assgnt
104 m				$\delta(\text{SHgS})$	100 m		100 m		$\delta(\text{HgS}_2)$
120 w		115 s		$\delta(\text{HgSC})$	224 w		172 <sup>b</sup> s		$\delta(\text{CS})$ , $\nu_s(\text{Hg-S})$
145 w				$\delta'(\text{HgS}_2)$	278 m		243 vw		$\tau(\text{NCH}_3)$
184 vw		191 m		$\delta_{\text{as}}(\text{CS})$ , $\nu_{\text{as}}(\text{Hg-S})$	317 w		323 m		$\delta(\text{CS})$ , $\rho(\text{NC}_2')$
		256 w		$\delta(\text{CS})$ , $\nu_s(\text{Hg-S})$	364 s		323 m		$\nu_{\text{as}}(\text{Hg-S})$
		360 s		$\nu_s(\text{Hg-S})$			364 s		$\nu_s(\text{Hg-S})$
371 vw				$\nu_{\text{as}}(\text{Hg-S})$	406 s		408 w		$\gamma(\text{C}'\text{N})$
382 s		411 w		$\gamma(\text{C}'\text{N})$	460 w		460 w		$\sigma(\text{NC}_2')$ , $\rho(\text{NC}_2')$
414 m		430 vw		$\sigma(\text{NC}_2')$ , $\rho(\text{NC}_2')$	460 w		460 vw		$\delta(\text{ClO}_4)^f$
429 s		458 m		$\delta(\text{ClO}_4)$			516 m		$\sigma(\text{NC}_2')$ , $\delta(\text{CS})$
457 m		514 m		$\sigma(\text{NC}_2')$ , $\delta(\text{CS})$			931 m		$\nu_s(\text{ClO}_4)^f$
515 s		918 m		$\nu(\text{CS})^c$			967 m		$\nu(\text{CS})^e$

<sup>a</sup> Intensities: vs = very strong, s = strong, m = medium, w = weak, vw = very weak. Assignment:  $\delta$  = deformation,  $\gamma$  = out of plane bending,  $\tau$  = twisting,  $\rho$  = rocking,  $\sigma$  = scissoring,  $\omega$  = wagging. C' denotes methyl carbon and sh = shoulder. <sup>b</sup> Polarized Raman band. <sup>c</sup> Reference 47. <sup>d</sup> Coordinated ligand. <sup>e</sup> From some remaining liquid. <sup>f</sup> Reference 48. <sup>g</sup> All bands in the range between 100 and 500  $\text{cm}^{-1}$ , together with selected Raman bands below 1000  $\text{cm}^{-1}$  are given.

by Ueyama *et al.*<sup>49</sup> Zn–S stretching contributes to both the bands observed at 200 and 350 cm<sup>-1</sup> for this thiophenolate complex. The present *N,N*-dimethylthioformamide complex resembles the thiophenolate in having two similar bands at 178 and 335 cm<sup>-1</sup>; cf. Figures 4 and 5. The lower wavenumber band is more polarized in the Raman spectrum, indicating a larger contribution from symmetric Zn–S stretching. A probable assignment for the 178 cm<sup>-1</sup> band of the [Zn(SCHN(CH<sub>3</sub>)<sub>2</sub>)<sub>4</sub>](CF<sub>3</sub>SO<sub>3</sub>)<sub>2</sub> compound is symmetric Zn–S stretching coupled with ligand vibrations, mostly S–C deformation, and for the 335 cm<sup>-1</sup> band Zn–S stretching with some ligand contribution. The S–Zn–S bending should give rise to a low transition frequency in the solid state, probably the 130 cm<sup>-1</sup> band.

The Cd–S stretching bands are not as well defined as for the zinc ion, but the new bands appearing at 300 cm<sup>-1</sup> and at 390–400 cm<sup>-1</sup>, see Figure 4, can tentatively be assigned as the Cd–S symmetric and asymmetric stretching modes, respectively, and the bending mode to the 150–160 cm<sup>-1</sup> band; see Table 3. There is a difference of about 10 cm<sup>-1</sup> between the two different solid cadmium structures both for the bending and the higher stretching frequencies; cf. Figures 4 and 5. The shift is in the opposite direction as that expected from the shortening of the Cd–S bonds in the [Cd(SCHN(CH<sub>3</sub>)<sub>2</sub>)<sub>4</sub>(O<sub>3</sub>S<sub>2</sub>CF<sub>3</sub>)<sub>2</sub>] compound and suggests that the corresponding normal modes have substantial and different contributions of ligand vibrations in the two compounds.

**Metal–Ligand Coordination.** The vibrational transition frequencies are sensitive to changes in bond strength. Force constants are often used for relative comparisons of the bonding between different metal atoms to the same ligands. The stretching force constant,  $F_r$ , is proportional to the square of the symmetric stretching frequency,  $\nu^2$ , for the same effective mass of the ligands assuming harmonic vibrations and neglecting ligand–ligand interactions around the stationary metal atom.<sup>50</sup> In such comparisons for six-coordinated zinc, cadmium, and mercury(II) ions in the solvents water and dimethyl sulfoxide, the  $F_r$  values of cadmium are lower than those for zinc and mercury(II).<sup>5</sup> This is consistent with a more covalent bonding at least for the mercury(II) ion because it has a larger size than cadmium in comparable hexasolvates. Such a simplified comparison is not meaningful for the *N,N*-dimethylthioformamide solvates because of the different coordination numbers and the coupled modes.

There are several reasons for the decrease in coordination number from 6 found for cadmium to 4 for solvates of mercury(II) and zinc with strongly coordinating ligands. As discussed in a theoretical study the difference in covalency is expected to increase for a soft sulfur donor.<sup>13</sup> For mercury(II), and to some extent for zinc, the energy of the  $d_{z^2}$  orbital is close enough to the  $s$  and  $p$  orbitals in the valence shell to allow a noticeable mixing in the molecular orbitals of octahedral complexes by vibronic coupling,<sup>13</sup> also called second-order Jahn–Teller effect. The effect is an increase in the amplitude of the stretching vibration belonging to the  $E_g$  symmetry species in point group  $O_h$  and causes a tetragonal distortion of the octahedral coordination geometry.<sup>51</sup> With strongly coordinating ligands the destabilization of the six-coordination increases<sup>13</sup> and is probably

responsible for the change to four-coordination observed for the solvated mercury(II) ion in solutions of *N,N*-dimethylthioformamide and in liquid ammonia.<sup>52</sup> The high  $D_S$  values of these solvents, 52 and 69, respectively, represent their strong donor ability toward mercury(II).<sup>53</sup> Also in the solid state preliminary results from a crystal structure determination of [Hg(NH<sub>3</sub>)<sub>4</sub>](ClO<sub>4</sub>)<sub>2</sub> show four-coordination with a distorted tetrahedral coordination geometry for the solvated mercury(II) atom.<sup>54</sup>

The importance of the donor strength is evident from a comparison with the weaker nitrogen donor pyridine,  $D_S = 38$ . Even though it is a more bulky ligand, tetragonally elongated octahedral six-coordination is maintained around the solvated mercury(II) atom in the solid compound [Hg(NC<sub>5</sub>N<sub>5</sub>)<sub>6</sub>](CF<sub>3</sub>SO<sub>3</sub>)<sub>2</sub>.<sup>7</sup>

Vibrational coupling with  $d$ -orbitals also occurs in four-coordinated complexes although with less predictable distortion effects<sup>51</sup> and is the probable reason for the distorted tetrahedral geometries observed at mercury(II) atoms not only for the [Hg(SCHN(CH<sub>3</sub>)<sub>2</sub>)<sub>4</sub>]<sup>2+</sup> species in solution but also for the sulfur donor complexes in the solid state discussed above (see Large-Angle X-ray Scattering).

The most characteristic coordination geometry of mercury(II) is the formation of two strong collinear bonds, often occurring in the solid state with some weak equatorial secondary bonds as in the [Hg(SCHN(CH<sub>3</sub>)<sub>2</sub>)<sub>2</sub>](ClO<sub>4</sub>)<sub>2</sub> structure.<sup>16</sup> Moreover, mercury(II) *N,N*-diethyldithiocarbamate crystallizes simultaneously in two forms, denoted  $\alpha$  and  $\beta$ , from acetone solution.<sup>37</sup> The  $\alpha$ -form has a distorted tetrahedral structure with a mean Hg–S bond distance of 2.57 Å, while the centrosymmetric  $\beta$ -structure has two short Hg–S bonds at 2.398(4) Å and four more distant S atoms at 2.99 and 3.31 Å, showing the small energy difference between the two types of coordination geometry. The linear two-coordination with its weak secondary bonds can also be described as a static deformation of regular six-coordination by a second-order Jahn–Teller effect and is common for mercury(II) when ligands of different donor strength are present. This applies for geometric reasons also to the bidentate *N,N*-diethyldithiocarbamate ion as ligand. However, with an excess of monodentate strongly coordinating neutral or charged ligands or solvent molecules in solution, tetrahedral four-coordination always seems to be the most stable ligand arrangement around mercury(II), albeit easily distorted.

For a six-coordinated zinc ion the destabilizing by vibronic coupling is weaker than for mercury(II),<sup>13</sup> but the steric ligand–ligand repulsion is stronger for the smaller zinc ion. The balance between these two effects is evident for the small but strongly coordinating ammonia ligand, for which both tetra- and hexaamminezinc solvates have been characterized in the solid state.<sup>40,55</sup> In liquid ammonia zinc ions are four-coordinated, but hexaamminezinc(II) salts can be crystallized from the solutions, as for cadmium.<sup>41,56</sup> Since the solvated cadmium ion is six-coordinated in liquid ammonia,<sup>41,52</sup> the same type of coordination change takes place for similar electronic reasons as for the present *N,N*-dimethylthioformamide solutions, with the zinc and mercury(II) ions tetrahedrally and cadmium octahedrally solvated. For the solvated zinc ion the stronger

(49) Ueyama, N.; Sugawara, T.; Sasaki, K.; Nakamura, A.; Yamashita, Y.; Wakatsuki, S.; Yamazaki, H.; Yasuoka, N. *Inorg. Chem.* **1988**, *27*, 741.

(50) Jones, H. L. *Inorganic Vibrational Spectroscopy*; Marcel Dekker: New York, 1971; Chapter 3.

(51) Bersuker, I. B. *Electronic Structure and Properties of Transition Metal Compounds*; Wiley-Interscience: New York, 1996; Chapters 7.3 and 9.4.

(52) Chingakule, D. D. K.; Gans, P.; Gill, B. J. *J. Chem. Soc., Dalton Trans.* **1991**, 1329.

(53) Sandström, M.; Persson, I.; Persson, P. *Acta Chem. Scand.* **1990**, *44*, 653.

(54) Persson, I.; Sandström, M.; Stålhandske, C. I. Unpublished data.

(55) Yamaguchi, T.; Lindquist, O. *Acta Chem. Scand., Ser. A* **1981**, *35*, 811.

(56) Patil, K. C.; Verneker, V. R.; Jain, S. R. *Thermochim. Acta* **1976**, *15*, 257.



steric repulsion between the more bulky *N,N*-dimethylthioformamide ligands shifts the balance to four-coordination also in the solid state. However, an EXAFS study of the smaller nickel(II) ion in *N,N*-dimethylthioformamide solution gives the Ni–S distance 2.45 Å, consistent with a coordination of six solvent molecules.<sup>43</sup> As the ionic radius in six-coordination is 0.69, 0.74, and 0.78 Å for Ni<sup>2+</sup>, Zn<sup>2+</sup>, and high-spin Fe<sup>2+</sup>, respectively,<sup>57</sup> this comparison with the smaller, yet six-coordinated,

Ni<sup>2+</sup> ion shows that steric ligand–ligand repulsion only is not sufficient to cause the lower coordination number of zinc in the *N,N*-dimethylthioformamide solvates. The decisive factor is the vibronic coupling giving d-orbital participation in the bonding.

**Acknowledgment.** The financial support given by the Swedish Natural Science Research Council is gratefully acknowledged.

---

(57) Shannon, R. *Acta Crystallogr., Sect. A* **1976**, 32, 751.